Applied Ocean Research 100 (2020) 102155

Contents lists available at ScienceDirect

Applied Ocean Research

journal homepage: www.elsevier.com/locate/apor

A comprehensive path planning framework for patrolling marine environment

Xiao Zhou[a,b,c], Liang Cheng[a,b,d,*], Weidong Li[c], Chuanrong Zhang[c], Fangli Zhang[e], Fanxuan Zeng[a,b], Zhaojin Yan[a,b], Xiaoguang Ruan[a,b], Manchun Li[a,b,d]

[a] School of Geography and Ocean Science, Nanjing University, Nanjing 210023, China
[b] Collaborative Innovation Center of South China Sea Studies, Nanjing, Jiangsu 210023, China
[c] Department of Geography, University of Connecticut, Storrs, CT 06269, USA
[d] Jiangsu Center for Collaborative Innovation in Geographical Information Resource Development and Application, Nanjing, Jiangsu 210023, China
[e] School of Geosciences, Yangtze University, Wuhan 430100, China

ARTICLE INFO

Keywords:
Patrol path planning
Multi-criteria decision analysis
GIS
Linear programming
Navigation safety

ABSTRACT

Ship navigation safety is a growing concern in maritime transportation and shipping industry. Rescue ship patrol is an important operation for improving navigation safety in the marine environment. This paper proposes a patrol path support framework, which incorporates multiple criteria decision making, geographical information system (GIS), and linear programming, to determine optimal paths for rescue ships on routine patrols. The proposed framework comprises three steps. First, a navigation risk index is created to estimate the rescue demand by using GIS-based multi-criteria decision analysis. Second, the patrol area of a rescue ship is identified based on a temporal accessibility model. Third, the optimal patrol path is determined by solving a linear programming problem. The northeastern South China Sea was taken as the area for a case study to demonstrate the usefulness of the proposed framework, and the optimum patrol path was identified successfully. The findings of this study may help the concerned authorities to develop maritime patrol path planning.

1. Introduction

Maritime transportation is crucial for the development of the global economy since approximately 90% of the world trade freight is transported by this way [1]. However, the increasing number of ships over time has resulted in the growth in the possibility of navigation accidents [2,3]. Despite the significant efforts to ensure navigation safety at sea, there are still a large number of accidents in the shipping industry [4]. Coastal countries have the responsibility of providing maritime search and rescue (SAR) services and ensuring the safe navigation of ships along their coastal lines [5]. Generally, when a ship is in distress and sends out signals for help, the emergency command center should dispatch rescue ships to help the caller after receiving the signal [6]. However, the possible failure of the radio wave technology due to exposure in disastrous weather and the long distance between the rescue base and the ship in trouble may hinder a fast rescue response [7,8]. Therefore, it is crucial to establish a rescue team patrolling on the sea to provide timely assistance [7]. Routine patrolling of rescue ships with strong disaster resistance is an important part of the SAR services on the sea to ensure the safety of traveling ships. To accomplish the patrolling tasks, the most important step is the patrol path planning, which aims to make the designed plan with the best patrol performance, that is, achieve maximum demand coverage [9].

Several previous studies analyzed path planning in the marine environment using diverse approaches. Table 1 presents the major path planning approaches in the literature [10,11]. Most of them were focused on making paths more efficient (e.g., save fuel and time) for the traveling ships [9,12]. For example, Park and Kim [13]applied the A* algorithm to determine the optimal plan at each time step with the aim to minimize fuel consumption. Yoo and Kim [14] proposed a route planning algorithm, which uses machine learning to obtain an ideal route for a marine vehicle by considering the impact of ocean current. Recently, Zaccone and Figari [15] used dynamic programming to select the route and speed of a ship in accordance with a minimum fuel consumption strategy. Similarly, Lee et al. [11] developed a cell-free technology for path planning, in which the navigation path and the speed of a ship can be determined concurrently. Furthermore, a multiple criteria sea path planning approach was presented very recently by Jeong et al. [9], which can objectively obtain the paths of ships according to their goals and preferences. However, studies that examine

* Corresponding author at: School of Geography and Ocean Science, Nanjing University, Nanjing, 210023, PR China.
E-mail address: lcheng@nju.edu.cn (L. Cheng).

https://doi.org/10.1016/j.apor.2020.102155
Received 2 January 2020; Received in revised form 2 March 2020; Accepted 31 March 2020

Table 1
Advantages and disadvantages of existing path planning methods.

Methods	Advantages	Disadvantages
Dijkstra algorithm [17]	Can find all optimal paths. Correct rate is high.	Computation time is long. Result path is not smooth.
A-star algorithm [18]	Computation time is not affectedby calculation precision. Computation time is relatively short.	Result may be a local optimum. Has limitations on searching direction.
Isochrone method [19]	Speed optimization is relatively easy. No limitation on searching direction.	Has limitations on the number of constraints and variables.
Dynamic programming [20]	Can easily handle strong nonlinearity and any type of constraints.	Has high computational cost and complexity.
Genetic algorithm [21]	Can solve multiple objectives.	Computational speed is still slow.
DIRECT Method [22]	Can search for both global and local optima simultaneously.	May take long time to find a local optimal route.

the patrol path planning are relatively few. One example is Yan et al. [16], which presented a path optimization technology for multi-autonomous underwater vehicles to determine an optimal path in a complicated environment. Another example is Huang et al. [7], which proposed an artificial immune algorithm to determine the optimal patrolling strategy for multi-robot systems. Although some progress has been made, analyzing these existing works revealed that they were mainly focused on designing or optimizing the path planning algorithms. In particular, there is no study on planning and visualizing the patrol paths for rescue ships, especially with the consideration of rescue demands, which is crucial for improving navigation safety.

In this study, we develop a patrol path support framework for determining the optimal path for a rescue ship on routine patrol. It attempts to incorporate multiple criteria decision making, geographical information system (GIS), and linear optimization into patrol path planning in the marine environment. The framework comprises three steps. First, a risk index is proposed to estimate the rescue demand by using GIS-based multi-criteria decision analysis. Then, a temporal accessibility model is structured to identify the patrol area. Finally, an optimal patrol path can be determined by solving a linear optimization model. To demonstrate the usefulness and applicability of the proposed framework, we conducted a case study in the northeast part of the South China Sea (SCS). The results of this study may help policymakers to develop better strategic plans for maritime SAR operations and improve navigation safety.

Overall, the contribution of this study is threefold: (1) we conduct a thorough literature review and establish a more comprehensive criteria system to evaluate the rescue demand in this study; (2) to the best of our knowledge, this is a first attempt to incorporate multi-criteria decision analysis, GIS, and linear optimization into patrol path planning in the marine environment, which is crucial for ensuring navigation safety; (3) we apply the proposed framework to a case study region in the northeastern SCS. The results obtained can help the concerned government to develop effective patrol strategies to protect crew and ships from the catastrophic influences of marine disasters. In addition, although the northeastern SCS is used as the case study area in this study, the proposed framework is applicable to any other sea area for identifying optimal patrol paths.

The remainder of this paper is organized as follows. Section 2 presents the methodological framework used in this study. In Section 3, the study area and the data are introduced. Sections 4 and 5 present the results and discussion, respectively. In Section 6, the conclusions are summarized, and the limitations of this study are presented.

2. Methods

The methodological framework for supporting maritime patrol path planning is shown in Fig. 1. In Step 1, the risk-based rescue demand index is evaluated. Step 2 identifies the patrol area. The optimal patrol path is determined for maritime SAR services in Step 3.

2.1. Risk-based demand index evaluation

The patrol path of rescue ships is expected to provide broader coverage of rescue demand. In this case, it is the first step to calculate the potential incident locations that could indicate the stochasticity of demand in the future [23]. Risk is regarded as the possibility of the occurrence of accidents, which can be introduced to describe the potential rescue demand [5,24]. In this study, GIS-based multi-criteria decision analysis, which solves spatial problems by weighting different spatial criteria in the decision-making process [25], was used to create the risk index.

2.1.1. Risk evaluation criteria

Regarding navigational risk, many researches from qualitative assessments to quantitative assessments have been conducted [26]. According to the existing literature (e.g., [27] and [28]), risk can be defined as a function of hazard, vulnerability and exposure, and it is calculated as follows:

$$Risk = Hazard \times Vulnerability \times Exposure \quad (1)$$

(1) Hazard criteria

Hazard is described as a natural or man-made event that may result in loss of life, property damage, and environmental pollution [29]. Ship navigation safety is threatened by various types of hazards. Following an extensive review of the published literature [30–36], eight criteria were used to describe the hazards for ship navigation, including water depth, gale frequency; big wave frequency, fog, precipitation, typhoon pressure, typhoon frequency, and piracy and armed robbery frequency, as shown in Table 2.

(2) Vulnerability and exposure criteria

In this study, vulnerability and exposure are grouped together due to the complexly related properties of a system [37]. They define the degree of loss of a system caused by hazards, which depends on the properties of the hazard events and their interactions with the characteristics of the system [38,39]. Totally, four criteria were chosen for evaluating vulnerability and exposure, and they concerned mainly the physical aspect, as shown in Table 2. More precisely, the vulnerability criteria include proximity to coastline, proximity to port, and proximity to sea route. The exposure criterion is ship density. It can be considered as the degree of exposure of ships to marine hazards. Increasing ship density implies more interactions between ships and possible hazards. Therefore, risk will increase due to greater exposure [40].

2.1.2. Weight calculation

The Analytical Hierarchy Process (AHP) technique was applied to weight each criterion in this study. Many multiple criteria decision-making methods have been developed, but the AHP is the most used to solve complex decisions with different criteria [45,46].

At the beginning of each AHP process, a pairwise comparison matrix

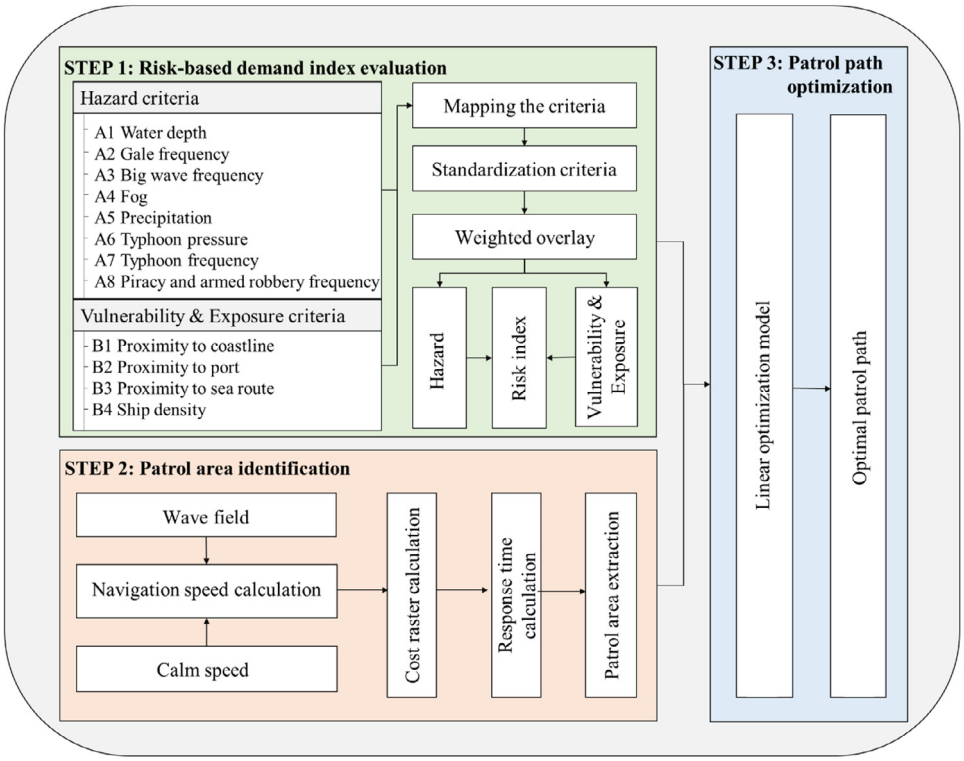

Fig. 1. The methodological framework for maritime patrol path planning support.

A is first created to estimate ratio scales, in which each entry c_{ij} in the matrix is built by comparing the relative importance of criterion C_i over criterion C_j. The pairwise comparison matrix A is given as follows [47]:

$$A = \begin{bmatrix} c_{11} & c_{12} & \cdots & c_{1n} \\ c_{21} & c_{22} & \ldots & c_{2n} \\ \vdots & \vdots & \ddots & \vdots \\ c_{n1} & c_{n2} & \cdots & c_{nn} \end{bmatrix} \quad (2)$$

According to Saaty [45], the fundamental 9-point scale was used to create a pairwise comparison matrix. The scale is explained in Table 3. The weight of each criterion could be estimated by calculating the principal eigenvector of the pairwise comparison matrix as follows:

$$Aw = \lambda_{max} w \quad (3)$$

where A is the pairwise comparison matrix, w is the principal eigenvector, and λ_{max} is the maximal eigenvalue. The weights of the criteria are obtained by normalizing w.

Because the pairwise comparisons of criteria can be inconsistent, the consistency relationship (CR) was further introduced to justify the degree of consistency of comparison matrices. If the CR is equal or less than 0.1, the comparisons are considered consistent. To obtain the CR, the consistency index (CI) is first calculated as follows:

$$CI = \frac{(\lambda_{max} - n)}{n - 1} \quad (4)$$

where λ_{max} is the largest eigenvalue, and n indicates the number of attributes [48].

Then, the CR can be calculated by using the following equation:

$$CR = \frac{CI}{RI} \quad (5)$$

where RI is the random index.

2.1.3. Rescue demand estimation

A grid cell of 1 km by 1 km was produced for each criterion to apply the weighted overlay technique. To conduct the multi-criteria decision on the same scale, all spatial criteria were standardized into the same scale from 0 to 1 by applying the following equation [49].

$$V = \begin{cases} \dfrac{V_{value} - V_{\min}}{V_{\max} - V_{\min}}, & \text{if } V \text{ is a positive variable} \\ \dfrac{V_{\max} - V_{value}}{V_{\max} - V_{\min}}, & \text{if } V \text{ is a negative variable} \end{cases} \quad (6)$$

where V is the standardized value, V_{max} and V_{min} is the maximum and minimum value of each criterion respectively, and V_{value} is the cell value.

Hazard index and vulnerability and exposure index were calculated individually by applying the weighted overlay technique in the ArcGIS platform. Then, the indices were categorized into fifteen classes for generating the hazard map and the vulnerability and exposure map. Finally, a risk index was created by following the risk Eq. (1). Similarly, the produced risk index was then classified into fifteen classes for producing a risk-based demand index map.

2.2. Patrol area identification

A patrol area is a geographic region of a sea where one or more rescue units are assigned. In general, a sea is often classified into several patrol regions with balanced workloads for providing better service [50]. In this study, a temporal accessibility model was developed to assess the response time of a maritime search and rescue system. Then, the patrol area for each rescue base is determined according to a specified response time. We divided the patrol area into two categories by setting a response time threshold: single patrol area and joint patrol area. The former means an area where the response time is less than the threshold and only one rescue base is responsible for conducting daily patrols. The latter defines an area where the response time is larger than the threshold and all rescue bases can provide services. In this study, the response time threshold was set to be four hours according to consultation with marine experts.

The response time for maritime SAR can be described as the

Table 2
Equations and description of selected criteria.

Components	Criteria	Equations	Descriptions
Hazard	Water depth	$WD_i=\begin{cases}0, & if\ water\ depth < -20\\ water\ depth\ value, & else\end{cases}$ where WD_i is the water depth value in grid i.	Water depth needs to satisfy the requirements for ship navigation safety, otherwise, low bathymetry would cause ship grounding. In this paper, the threshold was set to 20 m, showing the water depth that bigger than 20 m is considered safe for the ship navigation[32]. The minimum safe depth is set to 2 m.
	Gale frequency	$gf_{ij}=\begin{cases}1, & if\ wind\ speed > 11.7\\ 0, & else\end{cases}$ $GF_i=\frac{\sum_{j=1}^{n} gf_{ij}}{n}, j=1, 2, \ldots, n.$ where gf_{ij} is a binary variable for every grid i on day j; GF_i is the gale frequency in grid i; n is the total number of days.	Gale can cause the ship to drift sideways, thus to raise the width required for operation [41]. Here, a wind with a speed of higher than 11.7 m/s would be regarded as a gale [32].
	Big wave frequency	$bf_{ij}=\begin{cases}1, & if\ wave\ height > 6\\ 0, & else\end{cases}$ $BF_i=\frac{\sum_{j=1}^{n} bf_{ij}}{n}, j=1, 2, \ldots, n.$ where bf_{ij} is a binary variable for every grid i on day j; BF_i is the big wave frequency in grid i; n is the total number of days.	Big waves mostly influence heave, pitch, and yaw [41]. In this study, we defined any wave with a wave height of higher than 6 m as a big wave [32].
	Fog	$VI_i=\frac{\sum_{j=1}^{n} v_{ij}}{n}, j=1, 2, \ldots, n.$ where VI_i is the fog value in grid i; v_{ij} is the fraction of grid i covered by low-level clouds or fog on day j; n is the total number of days.	To assess the influence of visibility on ship navigation, factors such as fog, precipitation should be considered systematically [42]. Ship navigation in restricted visibility would increase the possibility of a collision or grounding.
	Precipitation	$P_i=\frac{\sum_{j=1}^{n} p_{ij}}{n}, j=1, 2, \ldots, n.$ where P_i is the precipitation value in grid$i$; p_{ij} is the precipitation on day j in grid i; n is the total number of days.	
	Typhoon pressure	$TP_i=\frac{\sum_{k=1}^{m} tp_{ik}}{m}, k=1, 2, \ldots, m.$ where TP_i is the typhoon pressure index value in grid i; tp_{ik} is the typhoon pressure value of typhoon k in grid i; m is the total number of typhoons.	With the increasing impact of climate change, typhoons are becoming stronger and bigger, causing a higher risk of the navigation of vessels in the ocean [43]. In this study, typhoon pressure and typhoon frequency were used to assess the influence of typhoon on ship navigation.
	Typhoon frequency	$tf_{ik}=\begin{cases}1, & if typhoon occurs\\ 0, & else\end{cases}$ $TF_i=\sum_{k=1}^{m} tf_{ik}, i=1, 2, \cdots, m.$ where tf_{ik} is a binary variable for every grid i when typhoon k occurred; TF_i is the typhoon frequencyin grid i; m is the total number of typhoons.	
	Piracy and armed robbery frequency	$pf_{ih}=\begin{cases}1, & if\ piracy\ and\ armed\ robbery\ occurs\\ 0, & else\end{cases}$ where pf_{ih} is a binary variable for every grid i when piracy and armed robbery h occurred; PF_i is the piracy and armed robbery frequencyin grid i; z is the total number of piracy and armed robbery occurrences. $PF_i=\sum_{h=1}^{z} pf_{ik},\ h=1, 2, \ldots, z.$	Piracy and armed robbery is the major anthropogenic hazard, which has emerged as one of the great threat to the safety of ship navigation [44].
Vulnerability and exposure	Proximity to coastline	Euclidean distance from coastline, port, and sea route respectively, calculated as follows: $D(c_q, c_p)=\sqrt{(x_q-x_p)^2+(y_q-y_p)^2}$ where (x_q,y_q) are the Cartesian coordinates point of c_q; (x_p,y_p) are the Cartesian coordinates point of c_p.	Ships near the areas including coastline, port, and sea route are highly vulnerable to hazard impacts than those far from such regions because of frequent society and economic activity [32].
	Proximity to port		
	Proximity to sea route		
	Ship density	$sd_{iu}=\begin{cases}1, & if\ ship\ u\ located\ in\ grid\ i\\ 0, & else\end{cases}$ where sd_{iu} is a binary variable for ship $u$in every grid i; $SD_i=\frac{\sum_{u=1}^{g} sd_{iu}}{A}, u=1, 2, \ldots, g$ SD_i is the ship density in grid i; A is the area of the grid; g is the total number of ships.	Frequent global trade has accelerated the development of maritime transportation. However, with bigger ship densities, there would be greater risks to ship navigation [5].

Table 3
Scales for pairwise comparison [45].

Numerical rating	Scale	Interpretation
1	Equal importance	Two activities contribute equally to objective
3	Moderate importance	Experience and judgment slightly favor one activity over another
5	Strong importance	Experience and judgment strongly favor one activity over another
7	Very strong importance	A criterion is favored strongly over another and its dominance is established in practice
9	Extreme importance	The evidence favoring one activity over another is of the highest possible order of validity
2, 4, 6, 8	Intermediate values between the two adjacent judgments	When compromise is needed

Table 4
Value of the coefficient *f*.

θ	Configuration name	f[kn/ft^2]
$0^\circ \le \theta \le 45^\circ$	Following seas	0.0083
$45^\circ < \theta < 135^\circ$	Beam seas	0.0165
$135^\circ \le \theta \le 180$	Head seas	0.0248

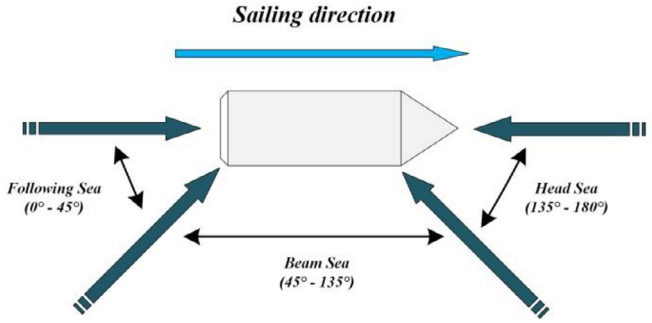

Fig. 2. The ship-wave relative direction.

minimum travel time from a rescue base to an incident site. The temporal accessibility model includes the following two steps: (a) calculation of the actual ship's speed [51]; (b) calculation of the response time of the rescue ship. The response time is obtained by the following equation:

$$S_c = S_0 - f(\theta)H^2 \tag{7}$$

$$T_r = Min \sum_{c=1}^{M} \frac{L_c}{S_c} \tag{8}$$

where S_c represents the actual ship speed crossing cell c in the marine environment, S_0 represents the ship speed in calm water, and f represents the coefficient (Table 4). In addition, H represents the significant wave height, θ represents the ship-wave relative direction (Fig. 2),T_r represents the response time for maritime SAR, and L_c represents the distance crossing cell c, $c = 1, 2, \ldots, M$.

Generally, a rescue base has a series of rescue equipment, including offshore patrol vessels, towing vessels, medical ships, etc. [52]. In this study, a patrol vessel called Huaying was assigned to do patrols away from the coast because this vessel provided maritime SAR services frequently. Its top speed can reach 20–30 knots and its patrol range is about 200–300 nautical miles. Here, cost distance analysis, which is a GIS-based technology, was used to obtain the rescue vessel's response time.

2.3. Patrol path optimization

The optimization model used in this study is a linear programming problem, which determines the optimal path for a rescue ship on routine patrols. The objective of the linear programming model is to achieve maximum demand coverage with respect to voyage constraints. We assumed that the rescue demand of one grid cell is covered by a patrol when the patrol path passes through the grid cell. A patrol path is divided into two sections including a coming path and a return path. The former represents the path that the rescue ship sails from a rescue base to the location of a turning point that the rescue ship decides to return. The latter indicates the path that the rescue ship returns to the rescue base from the location of the turning point.

In this context, a linear programming formulation is given as follows:

$$Max\ z = \sum_{i,j \in N} R_{ij}x_{ij} + \sum_{i,j \in N} R_{ij}y_{ij} \tag{9}$$

s.t.

$$\sum_{i,j \in N} x_{ij} + \sum_{i,j \in N} y_{ij} = L \tag{10}$$

$$x_{ij} * y_{ij} = 0 \tag{11}$$

$$x_{ij} = \begin{cases} 1, & if\ coming\ to\ cell\ (i,j) \\ 0, & otherwise \end{cases} \tag{12}$$

$$y_{ij} = \begin{cases} 1, & if\ return\ to\ cell\ (i,\ j) \\ 0, & otherwise \end{cases} \tag{13}$$

where i and j are the coordinate indices of a cell (i, j), N represents the set of cells available, R_{ij}represents the rescue demand at the cell (i, j), x_{ij}represents a binary variable for every cell (i, j) on the coming path, y_{ij}represents a binary variable for every cell (i, j) on the return path, and L is the ship's range.

The objective function (9) maximizes the coverage of rescue demand with respect to voyage constraints. Constraint (10) implies that the range of the coming path plus the range of the return path is equal to the ship's range set by a decision-maker. Constraint (11) means that one cell only can belong to one path (coming path or return path). Constraints (12) restricts x_{ij} to one only if the coming path passes through the cell (i, j). Constraints (13) restricts y_{ij} to one only if the return path passes through the cell (i, j).

The Least-Cost Path algorithm within a GIS framework was applied as a foundation to solve the proposed linear programming model. This algorithm has widespread applications, such as designing recreational trails [53], determining travel distances between communities [54], generating wildlife corridors [55], and optimizing electricity transmission lines [56]. It works by finding a connected path of cells in a cost raster that generates a least-cost path between a start point and an end point [57]. Three steps are included in the computation process in ArcGIS software [57,58]. First, the cost value is calculated for each cell. The cost value may represent time, distance, difficulty, or risk, to move across a cell. Next, the cumulative cost values between a specified origin cell and each of other cells are calculated by using the COSTDISTANCE function, thus to create an accumulated cost surface. The final step is to apply the COSTPATH function to identify the least cost path between a specified destination and a start point crossing the accumulated cost surface by minimizing the sum of the cost values included in the path. In this study, cost raster is the reciprocal of the rescue demand layer. It is noted that we modified the objective function in order to better apply the Least-Cost Path algorithm in the calculation process, as follow:

$$Min\ F = 1/\ z \tag{14}$$

where F is the reciprocal of parameter Z.

The Model Builder tool provided by the ArcGIS software (v.10.3) was used to conduct this calculation process. The created model based on Model Builder is shown in Fig. 3.

3. Case study

To demonstrate the usefulness and applicability of the proposed framework for supporting maritime patrol path planning, a case study is presented below.

3.1. Study area

This study was conducted in the northeastern SCS as shown in Fig. 4. It is one of the most heavily traveled sea areas in the world, with a large number of ports along the coasts. Some of these ports are world-class ports, such as Shenzhen port, Guangzhou port, and Hong Kong port [59]. However, this sea area is also known as a “dangerous sea area” since ship accidents occur frequently [5]. For better providing

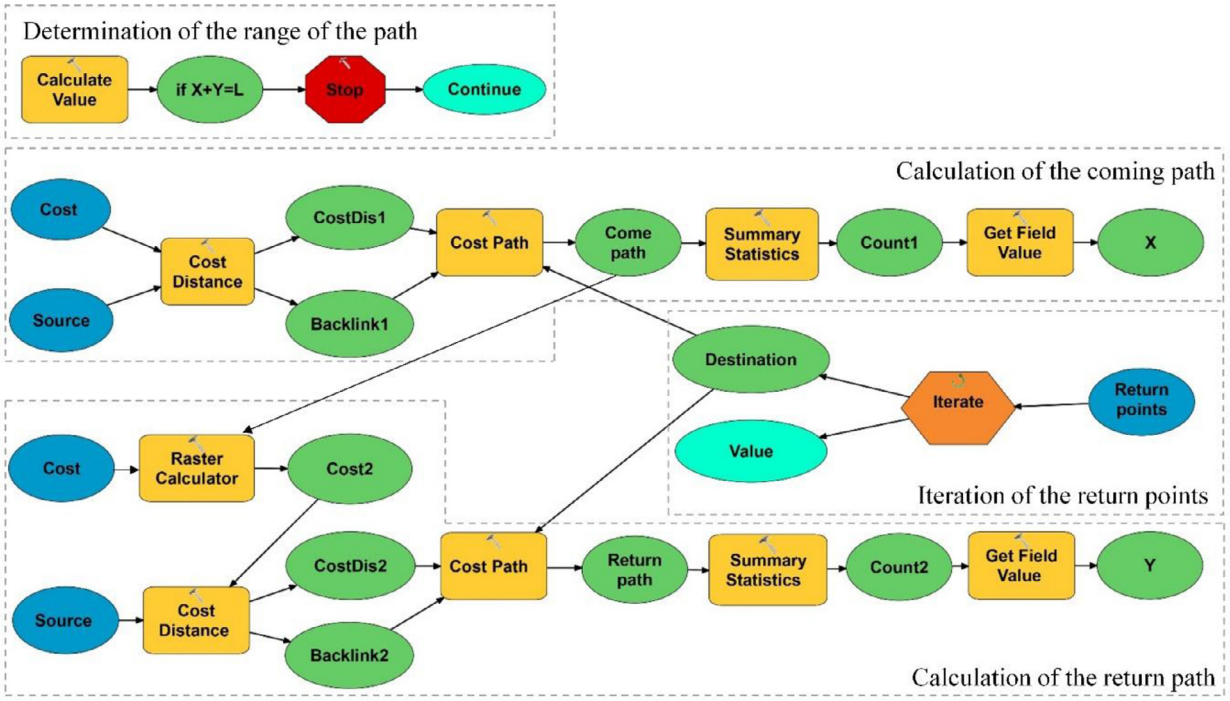

Fig. 3. Flowchart of model builder.

maritime SAR services, the Chinese government has established the Nanhai Rescue Bureau for providing maritime SAR services, which includes eight rescue bases, such as Guangzhou rescue base, Shantou rescue base, Shenzhen rescue base, Yang jiang rescue base, etc. (see Fig. 4).

3.2. Data collection

The data used in this study are as follows:

(1) Water depth. Water depth data were collected from the General Bathymetric Chart of the Oceans (https://www.gebco.net/) issued in 2019.
(2) Typhoon data. Typhoon data recorded from 1980 to 2018 were obtained from the online portal of the International Best Track Archive for Climate Stewardship (https://www.ncdc.noaa.gov/ibtracs/).
(3) Wind, wave, low-level cloud, and precipitation data. The data on fog, wind, wave, and precipitation recorded from 2004 to 2018 were collected from the European center for Medium-Range Weather Forecasts (https://www.ecmwf.int). Due to the lack of sea fog data, the low-level cloud data was used to calculate fog density [60].
(4) Piracy and armed robbery data. Piracy and armed robbery data from 1999 to 2018 were obtained from the Global Integrated Shipping Information System (https://gisis.imo.org/).
(5) Marine casualties and incidents data. Marine casualties and incidents data from 2013 to 2018 were collected from the Global Integrated Shipping Information System (https://gisis.imo.org/).
(6) Ship location data. The information for ship locations in 2017 was obtained from the Automatic Identification System Data (http://www.shipxy.com/).

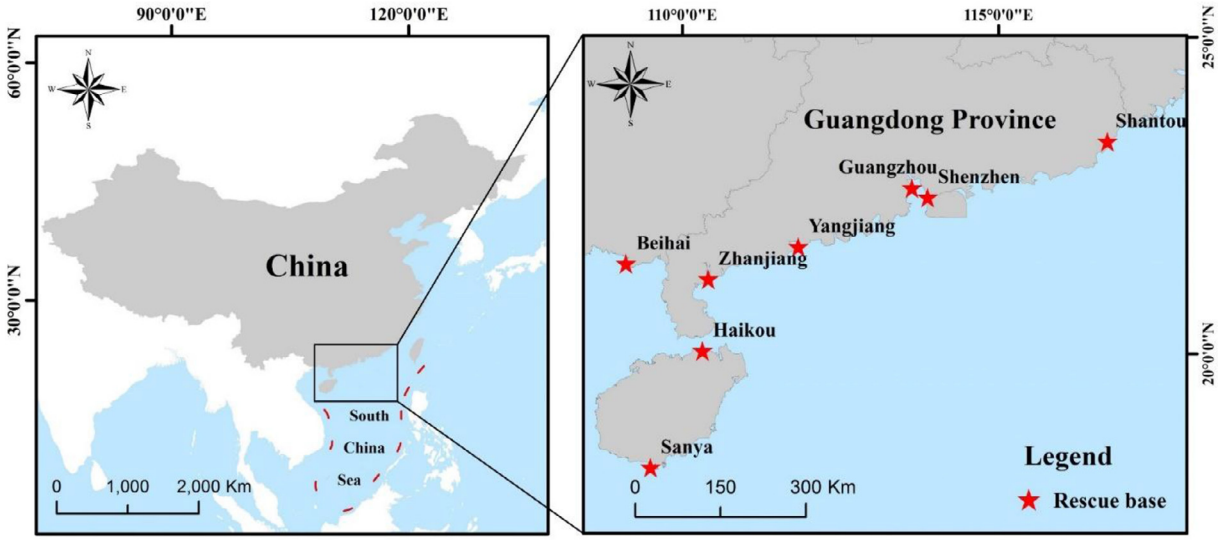

Fig. 4. Location of the study area.

Table 5
The pairwise comparison matrix with regard to hazard.

Hazard	Water depth	Typhoon pressure	Typhoon frequency	Fog	Big wave frequency	Gale frequency	Precipitation	Piracy and armed robbery frequency
Water depth	1	1/2	1/2	2	2	2	3	3
Typhoon pressure	2	1	2	3	2	2	2	3
Typhoon frequency	2	1/2	1	3	2	2	2	3
Fog	1/2	1/3	1/3	1	1/3	1/2	2	1
Big wave frequency	1/2	1/2	1/2	3	1	2	3	1
Gale frequency	1/2	1/2	1/2	2	1/2	1	2	1
Precipitation	1/3	1/2	1/2	1/2	1/3	1/2	1	1/2
Piracy and armed robbery frequency	1/3	1/3	1/3	1	1	1	2	1

(7) Coastline data. Coastline data were collected from the Global Self-consistent, Hierarchical, High-resolution Geography Database (https://www.ngdc.noaa.gov/mgg/shorelines/).
(8) Rescue base data. The data for rescue bases were obtained from the Nanhai Rescue Bureau of the Ministry of Transport of the People's Republic of China (http://www.nh-rescue.cn/).
(9) Port data. Port data were collected from the World seaports catalog, marine and seaports marketplace (http://ports.com/).
(10) Sea route data. Sea route data were collected from the Map of the World Oceans [61].

4. Results

4.1. AHP weights

In this study, five marine experts were invited to evaluate the intensity of preference between two factors according to Table 3 for creating the pairwise comparison matrix. Table 5 shows the pairwise comparison matrix with regard to hazard, and Table 6 indicates the pairwise comparison matrix with regard to vulnerability and exposure.

Then, using the AHP technique, the criterion weights and consistency ratios can be obtained as shown in Table 7. Obviously, the pairwise comparison matrix is considered as consistent since CR is equal to 0.04 and 0.02 respectively (lower than the threshold of 0.1).

4.2. Rescue demand

The maps shown in Fig. 5 give a better understanding of the spatial distribution of the rescue demand. The three indexes, namely hazard index, vulnerability and exposure index, and risk-based demand index, were all classified into fifteen classes. The sea area with a corresponding index value equal to or greater than 10 is considered a high hazard, vulnerability& exposure, or demand level. The hazard map illustrates the spatial variation of hazard in the northeastern SCS (Fig. 5a). It reveals that approximately 76.4% of the study area was located in a high hazard zone, that is, most areas are at high levels of hazard. Fig. 5b presents the spatial pattern of the vulnerability and exposure in the northeastern SCS. The results indicate that the area with a high level of vulnerability and exposure covered 39.4% of the study area. These regions were mostly located in coastal areas. Furthermore, the spatial variation and degree of rescue demand are shown in Fig. 5c. Approximately 33.5% of the study area was located in a zone with high rescue demand. It is clear that the coastal areas of the northeastern SCS had a higher rescue demand than those far from such areas.

Table 6
The pairwise comparison matrix with regard to vulnerability and exposure.

Vulnerability and exposure	Ship density	Proximity to coastline	Proximity to port	Proximity to sea route
Ship density	1	3	2	2
Proximity to coastline	1/3	1	1/2	1/2
Proximity to port	1/2	2	1	2
Proximity to sea route	1/2	2	1/2	1

Table 7
Criteria weights and consistency ratios.

Components	Criteria	Weight	Consistency Ratio
Hazard	Water depth	0.16	0.04
	Typhoon pressure	0.23	
	Typhoon frequency	0.19	
	Fog	0.07	
	Big wave frequency	0.12	
	Gale frequency	0.09	
	Precipitation	0.06	
	Piracy and armed robbery frequency	0.08	
Vulnerability and Exposure	Ship density	0.41	0.02
	Proximity to coastline	0.12	
	Proximity to port	0.27	
	Proximity to sea route	0.20	

4.3. Patrol area

A quick response corresponds to bigger chances for survival. Fig. 6a shows the response times of the maritime SAR system built at the northeastern SCS. Overall, response times from SAR bases to areas near the coast show greater efficiency than those in the area far away from the shoreline, which is almost less than 2 h as shown in Fig. 6a. Obviously, these coastal bases have improved the ability of short-distance maritime SAR, but long-distance maritime SAR still faces many challenges and should be improved. Furthermore, the studied sea area was classified into several patrol districts based on the response times of the maritime SAR system. In this study, the response time threshold was set to 4 h according to consultation with marine experts. And we used the Yangjiang base as a case study. Fig. 6b shows the patrol area of the Yangjiang base, which includes a single patrol area and a joint patrol area.

4.4. Patrol path

Using the Yangjiang base as an example, the optimal patrol path was determined, which is a closed curve. Its starting point and ending point are the same, namely the Yangjiang base. A patrol vessel called Huaying was assigned to do patrols away from the coast, and its calm speed was set to 30 knots. Fig. 7 shows the optimal patrol path where the ship's range is set to 150, 200 and 250 nautical miles, respectively. The patrol ship can achieve maximum demand coverage when navigating across the optimal patrol path. These three patrol paths are all located on the southeast side of the Yangjiang base, due to the higher rescue demand in these regions (see Fig. 5).

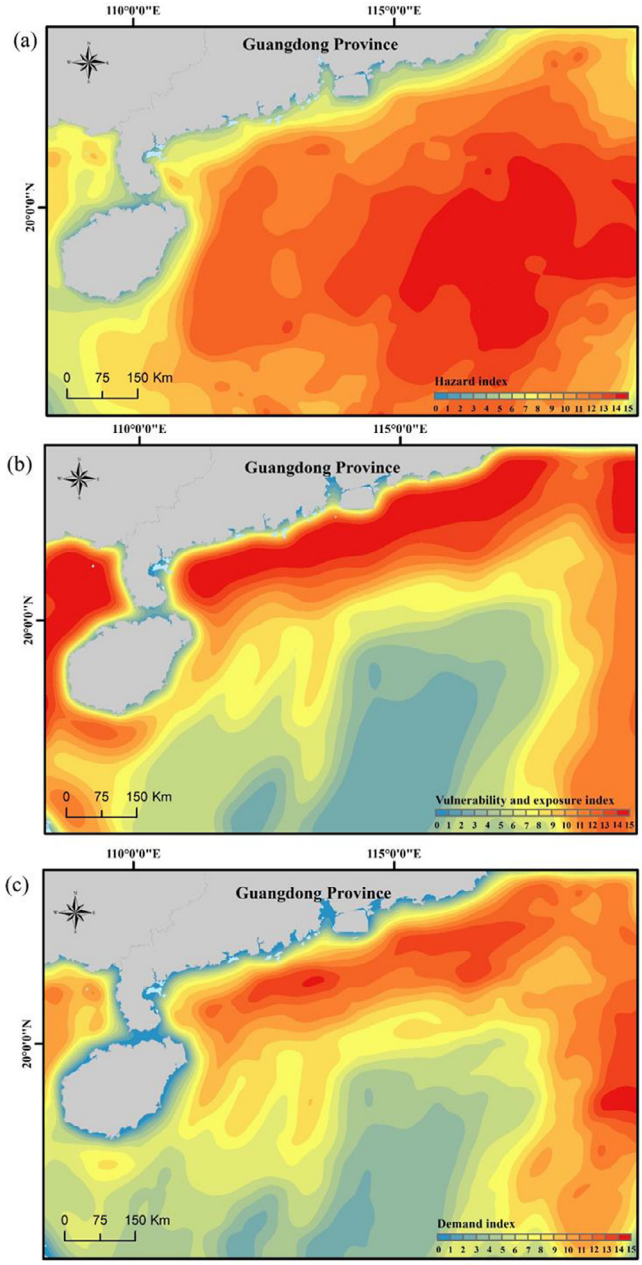

Fig. 5. Maps of the three indexes. (a) hazard index; (b) vulnerability & exposure index; (c) demand index.

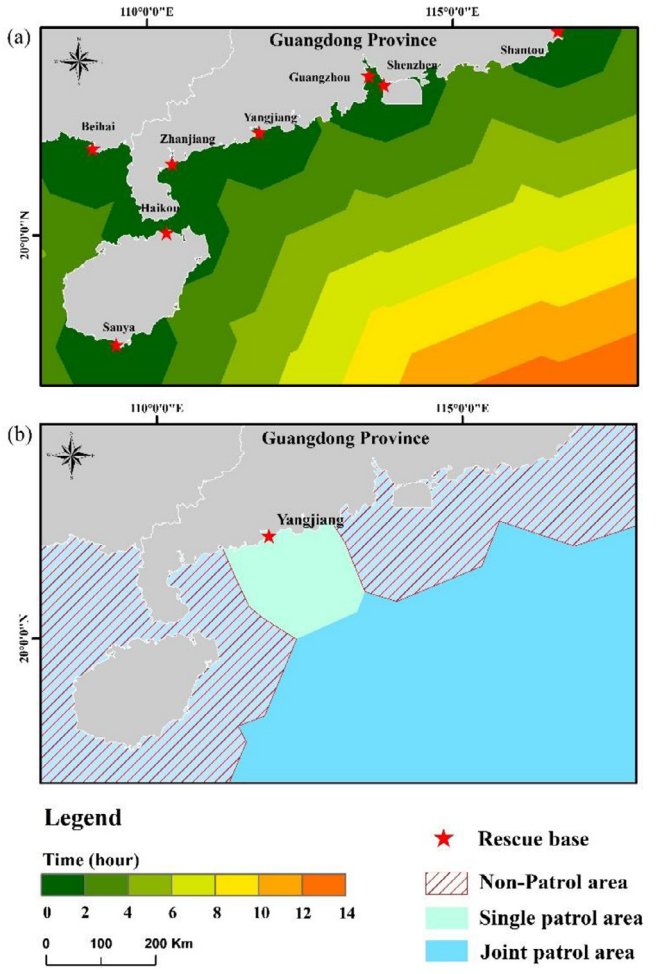

Fig. 6. Patrol area based on the response time of the maritime SAR system. (a) response time of the maritime SAR system; (b) patrol area of ships located in the Yangjiang base.

5. Discussion

In this study, we propose a path planning framework to support ship patrol at sea. Rescue demand estimation is the first step in the proposed framework. Its validation enables us to find whether the created approach is acceptable for its intended use. Therefore, 27 historical accidents obtained from the Global Integrated Shipping Information System were used to verify the produced risk index. The percentage of incidents in areas with risk index value equal to or greater than 10 was 85.2%.Such a percentage being more than 80% means that the evaluation results are valid [32].

The optimal patrol path for a patrolling vehicle is determined in this study. In fact, multiple SAR tasks can also be handled by using the proposed framework. The calculation process for handling multiple SAR tasks consists of two steps: (1) a path is first determined for one patrolling vehicle using the proposed method; (2) after excluding the first path area obtained in the first step from the candidate patrol area, the second path for another patrolling vehicle can be identified by the same method, and so on. In addition, the length of the patrol path can be different according to the capacity of the patrolling vehicle by setting the *range* parameter (i.e., L) of the ship in the proposed optimization model.

In addition, it is very challenging to obtain high-quality and up-to-date data for each criterion. In fact, most criteria used for this study are dynamic since their datasets are updated periodically. We required a wide variety of data from different national and international organizations. For example, the 0.125° resolution marine environment data, including wind, wave, low-cloud cover, and precipitation, were used in this study. Obviously, high-resolution data can improve data quality and provide better results [49]. However, it is impossible to improve data precision indefinitely, due to cost restraints or technical limitations [62].Furthermore, the grid size of the cell should be larger than the size of the rescue vehicle. In this study, the grid with 1 km × 1 km resolution was used in our study considering the trade-off between computation cost and accuracy [5]. In this context, the impact of the vehicle size on the results can be ignored. Especially, it also should be noted that the patrol path obtained by the proposed method has a few sharp or angular turns. Therefore, in a practical application, kinematic constraints of the ship should be further considered so that the patrolling vehicles can execute those turns and proceed as planned [63].

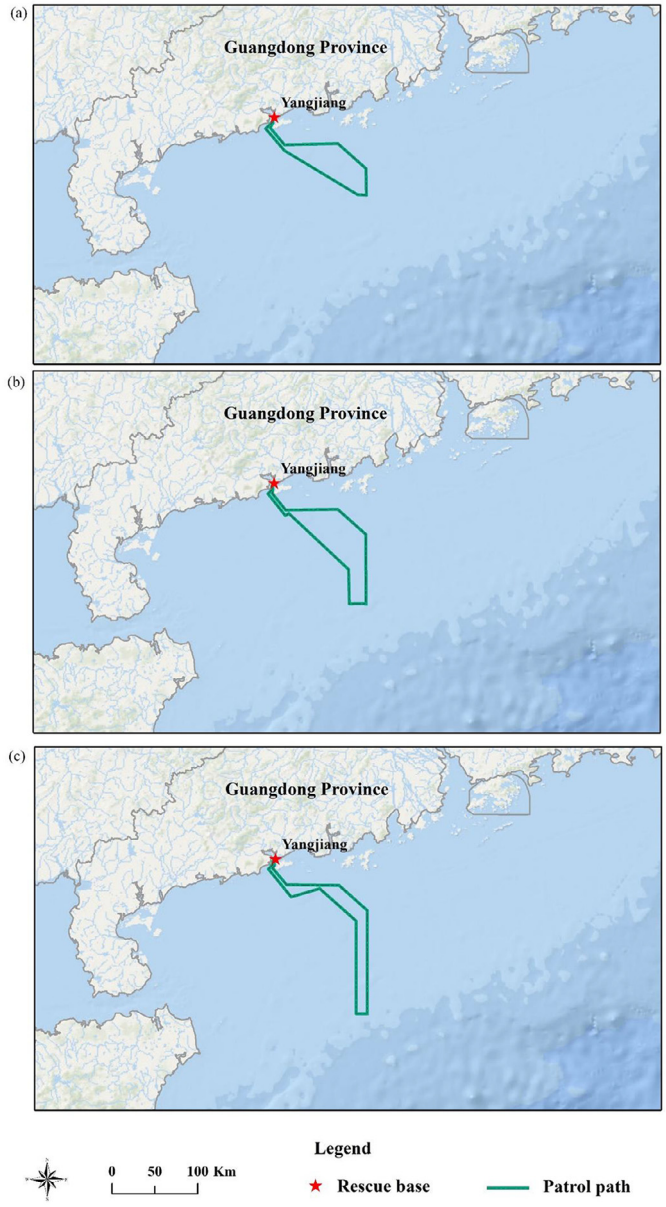

Fig. 7. Optimal patrol paths. (a) 150 nautical miles; (b) 200 nautical miles; (c) 250 nautical miles.

6. Conclusion

Maritime patrol is critical for ensuring navigation safety at sea. This paper proposes a comprehensive framework for supporting patrol path planning in the marine environment. Our study is the first attempt to determine the optimal paths for the rescue ships on routine patrols by integrating multiple criteria decision making, GIS, and linear programming. The framework comprises three steps. First, the rescue demand is identified by using a risk index. Second, a temporal accessibility model is constructed to identify a ship's patrol area. In the third step, an optimal patrol path is determined by solving the developed linear programming model. This framework was applied to the northeastern SCS, and optimal patrol paths were identified successfully. Our results can contribute to the current knowledge of patrol path planning in the marine environment, and provide new insights for the improvement of maritime navigation safety.

There are several limitations to this study. The actual ship speed was calculated by using a general ship speed model, which assumed that the speed reduction relies only on significant wave height and ship-wave relative direction. But other factors such as wind, current may also have an impact on the speed reduction. Therefore, future work should focus on developing a more accurate model that would provide better results. In addition, all rescue bases were considered as the same in our study. Differences in SAR equipment of each rescue base should be addressed in future study.

CRediT authorship contribution statement

Xiao Zhou: Conceptualization, Methodology, Validation, Formal analysis, Investigation, Writing - original draft, Writing - review & editing. **Liang Cheng:** Software, Data curation, Supervision, Funding acquisition. **Weidong Li:** Methodology, Writing - review & editing. **Chuanrong Zhang:** Visualization, Conceptualization. **Fangli Zhang:** Conceptualization. **Fanxuan Zeng:** Investigation. **Zhaojin Yan:** Investigation. **Xiaoguang Ruan:** Validation. **Manchun Li:** Software.

Declaration of Competing Interest

The authors declare that they have no known competing financial interests or personal relationships that could have appeared to influence the work reported in this paper.

Acknowledgments

This work was supported by the National Key R&D Program of China (No. 2017YFB0504205), the Guangxi Innovative Development Grand Grant (No. AA18118038), the National Natural Science Foundation of China (Nos. 41622109, 41371017), the Guangxi Key Laboratory of Spatial Information and Geomatics(No. 17-259-16-11), and the China Scholarship Council.

Supplementary materials

Supplementary material associated with this article can be found, in the online version, at doi:10.1016/j.apor.2020.102155.

References

[1] O.A.V. Banda, F. Goerlandt, J. Montewka, P. Kujala, A risk analysis of winter navigation in Finnish sea areas, Accident Anal. Prev 79 (2015) 100–116.
[2] Z. Liu, Z. Wu, Z. Zheng, A novel framework for regional collision risk identification based on AIS data, Appl. Ocean Res 89 (2019) 261–272.
[3] A.-.A. Baksh, R. Abbassi, V. Garaniya, F. Khan, Marine transportation risk assessment using Bayesian Network: application to Arctic waters, Ocean Eng 159 (2018) 422–436.
[4] S. Faghih-Roohi, M. Xie, K.M. Ng, Accident risk assessment in marine transportation via Markov modelling and Markov Chain Monte Carlo simulation, Ocean Eng 91 (2014) 363–370.
[5] X. Zhou, L. Cheng, F. Zhang, Z. Yan, X. Ruan, K. Min, M. Li, Integrating Island Spatial Information and Integer Optimization for Locating Maritime Search and Rescue Bases: a Case Study in the South China Sea, ISPRS Int. J. Geo-Inf 8 (2019) 88.
[6] H. Karahalios, The severity of shipboard communication failures in maritime emergencies: a risk management approach, Int. J. Disast. Risk Re 28 (2018) 1–9.
[7] L. Huang, M. Zhou, K. Hao, Non-dominated immune-endocrine short feedback algorithm for multi-robot maritime patrolling, IEEE T. Intell. Transp (2019) 1–12.
[8] J. Nordström, F. Goerlandt, J. Sarsama, P. Leppänen, M. Nissilä, P. Ruponen, T. Lübcke, S. Sonninen, Vessel TRIAGE: a method for assessing and communicating the safety status of vessels in maritime distress situations, Safety Sci 85 (2016) 117–129.
[9] M.G. Jeong, E.B. Lee, M. Lee, J.Y. Jung, Multi-criteria route planning with risk contour map for smart navigation, Ocean Eng 172 (2019) 72–85.
[10] L. Walther, A. Rizvanolli, M. Wendebourg, C. Jahn, Modeling and optimization algorithms in ship weather routing, Int. J. e-Navigation Marit. Econ 4 (2016) 31–45.
[11] S.M. Lee, M.I. Roh, K.S. Kim, H. Jung, J.J. Park, Method for a simultaneous determination of the path and the speed for ship route planning problems, Ocean Eng 157 (2018) 301–312.
[12] T. Dickson, H. Farr, D. Sear, J.I. Blake, Uncertainty in marine weather routing, Appl. Ocean Res 88 (2019) 138–146.
[13] J. Park, N. Kim, Two-phase approach to optimal weather routing using geometric programming, J. Mar. Sci. Tech 20 (2015) 679–688.
[14] B. Yoo, J. Kim, Path optimization for marine vehicles in ocean currents using

reinforcement learning, J, Mar. Sci. Tech. 21 (2016) 334–343.
[15] R. Zaccone, M. Figari, Energy efficient ship voyage planning by 3d dynamic programming, J, Ocean Technol. (2017) 12.
[16] Z. Yan, J. He, J. Li, An improved multi-AUV patrol path planning method, IEEE International Conference on Mechatronics and Automation (ICMA), 2017, IEEE, 2017, pp. 1930–1936.
[17] E.W. Dijkstra, A note on two problems in connexion with graphs, Numer. Math 1 (1959) 269–271.
[18] P.E. Hart, N.J. Nilsson, B. Raphael, A formal basis for the heuristic determination of minimum cost paths, IEEE Trans. Syst. Sci. Cybern 4 (1968) 100–107.
[19] G.L. Hanssen, R.W. James, Optimum ship routing, J. Navigation 13 (1960) 253–272.
[20] T.H. Cormen, C.E. Leiserson, R.L. Rivest, C. Stein, Introduction to Algorithms, MIT press, 2009.
[21] D. Goldberg, Genetic Algorithms in Search, Optimization & Machine Learning Addison-Wesley, Reading, Mass, 1989.
[22] D.R. Jones, C.D. Perttunen, B.E. Stuckman, Lipschitzian optimization without the Lipschitz constant, J, Optim. Theory Appl. 79 (1993) 157–181.
[23] A. Akbari, H. Eiselt, R. Pelot, A maritime search and rescue location analysis considering multiple criteria, with simulated demand, INFOR 56 (2018) 92–114.
[24] S. Hu, Q. Fang, H. Xia, Y. Xi, Formal safety assessment based on relative risks model in ship navigation, Reliab. Eng. Syst. Safe 92 (2007) 369–377.
[25] F. Veronesi, J. Schito, S. Grassi, M. Raubal, Automatic selection of weights for GIS-based multicriteria decision analysis: site selection of transmission towers as a case study, Appl. Geogr 83 (2017) 78–85.
[26] S. Zhang, Z. Jing, W. Li, L. Wang, D. Liu, T. Wang, Navigation risk assessment method based on flow conditions: a case study of the river reach between the Three Gorges Dam and the Gezhouba Dam, Ocean Eng 175 (2019) 71–79.
[27] H. Carrao, G. Naumann, P. Barbosa, Mapping global patterns of drought risk: an empirical framework based on sub-national estimates of hazard, exposure and vulnerability, Global Environ. Change 39 (2016) 108–124.
[28] A. Ahmadalipour, H. Moradkhani, A. Castelletti, N. Magliocca, Future drought risk in Africa: integrating vulnerability, climate change, and population growth, Sci. Total Environ 662 (2019) 672–686.
[29] P. Blaikie, T. Cannon, I. Davis, B. Wisner, At risk: Natural hazards, People's Vulnerability and Disasters, Routledge, 2005.
[30] K. Mokhtari, J. Ren, C. Roberts, J. Wang, Application of a generic bow-tie based risk analysis framework on risk management of sea ports and offshore terminals, J. hazard. Mater 192 (2011) 465–475.
[31] W.-K.K. Hsu, Ports' service attributes for ship navigation safety, Safety Sci 50 (2012) 244–252.
[32] J. Wang, M. Li, Y. Liu, H. Zhang, W. Zou, L. Cheng, Safety assessment of shipping routes in the South China Sea based on the fuzzy analytic hierarchy process, Safety Sci 62 (2014) 46–57.
[33] B. Sahin, S. Kum, Risk assessment of Arctic navigation by using improved fuzzy-AHP approach, Int. J. Marit. Eng 157 (2015) 241.
[34] D. Zhang, X. Yan, J. Zhang, Z. Yang, J. Wang, Use of fuzzy rule-based evidential reasoning approach in the navigational risk assessment of inland waterway transportation systems, Safety Sci 82 (2016) 352–360.
[35] B. Khan, F. Khan, B. Veitch, M. Yang, An operational risk analysis tool to analyze marine transportation in Arctic waters, Reliab. Eng. Syst. Safe 169 (2018) 485–502.
[36] Y.-F. Tian, L.-J. Chen, L.-W. Huang, J.-M. Mou, Featured risk evaluation of nautical navigational environment using a risk cloud model, J. Mar. Eng. Technol (2018) 1–15.
[37] P.M. Kelly, W.N. Adger, Theory and practice in assessing vulnerability to climate change andFacilitating adaptation, Climatic Change 47 (2000) 325–352.
[38] B. Smit, J. Wandel, Adaptation, adaptive capacity and vulnerability, Global Environ. Change 16 (2006) 282–292.
[39] M.A.-A. Hoque, B. Pradhan, N. Ahmed, S. Roy, Tropical cyclone risk assessment using geospatial techniques for the eastern coastal region of Bangladesh, Sci. Total Environ 692 (2019) 10–22.
[40] A.K. Debnath, H.C. Chin, M.M. Haque, Modelling port water collision risk using traffic conflicts, J. Navigation 64 (2011) 645–655.
[41] M.J. Briggs, L.E. Borgman, E. Bratteland, Probability assessment for deep-draft navigation channel design, Coast. Eng 48 (2003) 29–50.
[42] D. Jiang, G. Hao, L. Huang, D. Zhang, Use of cusp catastrophe for risk analysis of navigational environment: a case study of three gorges reservoir area, PLoS ONE 11 (2016) e0158482.
[43] C. Chen, S. Shiotani, K. Sasa, Numerical ship navigation based on weather and ocean simulation, Ocean Eng 69 (2013) 44–53.
[44] G.J. Lim, J. Cho, S. Bora, T. Biobaku, H. Parsaei, Models and computational algorithms for maritime risk analysis: a review, Ann. Oper. Res 271 (2018) 765–786.
[45] T.L. Saaty, Decision making with the analytic hierarchy process, Int. J. Serv. Sci 1 (2008) 83–98.
[46] A.A. Merrouni, F.E. Elalaoui, A. Mezrhab, A. Mezrhab, A. Ghennioui, Large scale PV sites selection by combining GIS and Analytical Hierarchy Process. Case study: eastern Morocco, Renew. Energ. 119 (2018) 863–873.
[47] T. Höfer, Y. Sunak, H. Siddique, R. Madlener, Wind farm siting using a spatial Analytic Hierarchy Process approach: a case study of the Städteregion Aachen, Appl. Energ 163 (2016) 222–243.
[48] M. Mahapatra, R. Ramakrishnan, A. Rajawat, Coastal vulnerability assessment using analytical hierarchical process for South Gujarat coast, India, Nat. Hazards 76 (2015) 139–159.
[49] M.A.-A. Hoque, S. Phinn, C. Roelfsema, I. Childs, Assessing tropical cyclone risks using geospatial techniques, Appl. Geogr. 98 (2018) 22–33.
[50] H. Chen, T. Cheng, X. Ye, Designing efficient and balanced police patrol districts on an urban street network, Int. J. Geogr. Inf. Sci 33 (2019) 269–290.
[51] G. Mannarini, G. Coppini, P. Oddo, N. Pinardi, A prototype of ship routing decision support system for an operational oceanographic service, TransNav Int. J. Mar. Navig. Saf. Sea Transp 7 (2013).
[52] W. Shi, F. Su, C. Zhou, A temporal accessibility model for assessing the ability of search and rescue in Nansha Islands, South China Sea, Ocean Coast. Manage 95 (2014) 46–52.
[53] A.M. Tomczyk, M. Ewertowski, Planning of recreational trails in protected areas: application of regression tree analysis and geographic information systems, Appl. Geogr 40 (2013) 129–139.
[54] K. Webster, J. Arroyo-Mora, O. Coomes, Y. Takasaki, C. Abizaid, A cost path and network analysis methodology to calculate distances along a complex river network in the Peruvian Amazon, Appl. Geogr 73 (2016) 13–25.
[55] T. Shirabe, Buffered or bundled, least-cost paths are not least-cost corridors: computational experiments on path-based and wide-path-based models for conservation corridor design and effective distance estimation, Ecol. Inform 44 (2018) 109–116.
[56] A.H.M. Santos, R.M. de Lima, C.R.S. Pereira, R. Osis, G.O.S. Medeiros, A.R. de Queiroz, B.K. Flauzino, A.R.P.C. Cardoso, L.C. Junior, R.A. dos Santos, Optimizing routing and tower spotting of electricity transmission lines: an integration of geographical data and engineering aspects into decision-making, Electr. Pow. Syst. Res 176 (2019) 105953.
[57] S.A. Snyder, J.H. Whitmore, I.E. Schneider, D.R. Becker, Ecological criteria, participant preferences and location models: a GIS approach toward ATV trail planning, Appl. Geogr. 28 (2008) 248–258.
[58] D. Becker, D. Andrés-Herrero, C. Willmes, G.C. Weniger, G. Bareth, Investigating the influence of different DEMs on GIS-based cost distance modeling for site catchment analysis of prehistoric sites in Andalusia, ISPRS Int. J. Geo-Inf 6 (2017) 36.
[59] X. Tian, L. Liu, S. Wang, Evolving competition between Hong Kong and Shenzhen ports, Marit. Policy Manag. 42 (2015) 729–745.
[60] V. Sathiyamoorthy, R. Arya, C. Kishtawal, Radiative characteristics of fog over the Indo-Gangetic Plains during northern winter, Clim. Dynam 47 (2016) 1793–1806.
[61] The World Factbook, Map of the World Oceans. https://legacy.lib.utexas.edu/maps/world_maps/world_oceans_2015.pdf, 2015(Accessed 2 November 2019).
[62] Y. Li, A. Brimicombe, M. Ralphs, Spatial data quality and sensitivity analysis in GIS and environmental modelling: the case of coastal oil spills, Comput. Environ. Urban 24 (2000) 95–108.
[63] A. Ravankar, A.A. Ravankar, Y. Kobayashi, Y. Hoshino, C.C. Peng, Path smoothing techniques in robot navigation: state-of-the-art, current and future challenges, Sensors 18 (2018) 3170.